Supplementary information

for

Realizing High-Efficiency TADF from a Low-Performing Cyanopyridine Emitter via symmetric coupling

Ashish K. Mazumdar, Bhaskar Chelleng, Svadha Devi, Gyana Prakash Nanda, Ganesh Manikandan, P Rajamalli*

Materials Research Centre, Indian Institute of Science (IISc) Bangalore, C. V. Raman Road, Bengaluru, 560012, Karnataka, India

Email: rajamalli@iisc.ac.in

Contents

1. Materials and methods

1.1 Chemicals

All chemicals were used as received unless otherwise stated. The chemicals were received from Sigma-Aldrich, Merck India and Alfa aesar.

1.2 Instrumentation

The ^{1}H and ^{13}C NMR spectra were recorded by using Bruker Avance 400 spectrometer. The HRMS were measured using MAT-95XL HRMS or MStation. The UV-visible absorption spectra were taken on a JASCO FP-8500 spectrometer. Fluorescence and Phosphorescence spectra were recorded on a Hitachi F-7100 spectrophotometer, with the 77 K Phosphorescence spectrum measured in Phosphorescence mode using a 25 ms delay after photoexcitation.[8]The time-resolved emission spectra and decays were recorded using an Edinburgh Instruments FS5 spectrometer equipped with a double monochromator for both excitation and emission, operating in right-angle geometry mode and the highly sensitive photomultiplier tube (RED PMT in Cooled Housing) positioned after a double emission monochromator. Photoluminescence lifetime is measured the integrated device in Edinburgh instrument FS5 model. The thermogravimetric analysis (TGA, PerkinElmer) was recorded under N_2 flow from room temperature to 600 ºC. The cyclic voltammetry measurement was carried out in deoxygenated dichloromethane (DCM) with 0.1 M tetrabutylammonium hexafluorophosphate (TBAP) as supporting electrolyte in a three-electrode system using BioLogic SP50 potentiostat (Biologic, France). Glassy Carbon, Platinum wire (Pt), and Ag/AgCl/KCl(saturated) were used as working, counter, and reference electrodes respectively. The scan rate was kept at 100 mV/s for the measurement.

2. Synthesis and Characterizations

2.1 Synthesis of 3-(3,6-di-tert-butyl-9H-carbazol-9-yl)picolinonitrile (tCzPyCN)

Compound tCzPyCN is a known compound.[4] However, for clarity, we are writing the procedure we utilized for synthesis.

Procedure: A mixture of 3-Fluoropicolinonitrile (FPyCN) (1 g, 8.19 mmol), tert-butyl carbazole(tCz) (2.29 g, 8.19 mmol), Cesium carbonate (3.2 g, 9.80 mmol), in dry DMF 5 ml was placed in a 50 ml sealed tube under nitrogen environment. The reaction was stirred at a temperature of 145 ºC for 24 h [Scheme 1]. After completion of the reaction, the mixture was extracted and dried using sodium sulphate, and then the solvent was removed under reduced pressure. The dried compound was then purified by silica gel column chromatography and eluted in 10% ethyl

acetate/n-hexane mixture to give the desired white color compound (yield=82%). ^{1}H NMR (400 MHz, $CDCl_3$) δ 8.82 (dd, *J* = 4.7, 1.5 Hz, 1H), 8.15 (d, *J* = 1.8 Hz, 2H), 7.96 (dd, *J* = 8.3, 1.5 Hz, 1H), 7.72 (dd, *J* = 8.3, 4.6 Hz, 1H), 7.49 (dd, *J* = 8.6, 1.9 Hz, 2H), 7.13 (d, *J* = 8.6 Hz, 2H), 1.47 (s, 18H). ^{13}C NMR (400 MHz, $CDCl_3$) δ 149.74, 144.49, 139.28, 138.91, 137.13, 133.06, 127.89, 124.44, 124.16, 116.84, 115.32, 109.09, 34.87, 32.00. HRMS (ESI-QTOF) m/z: $[M+H]^+$ calculated for $C_{26}H_{27}N_3$ 382.2205, found 382.2277.

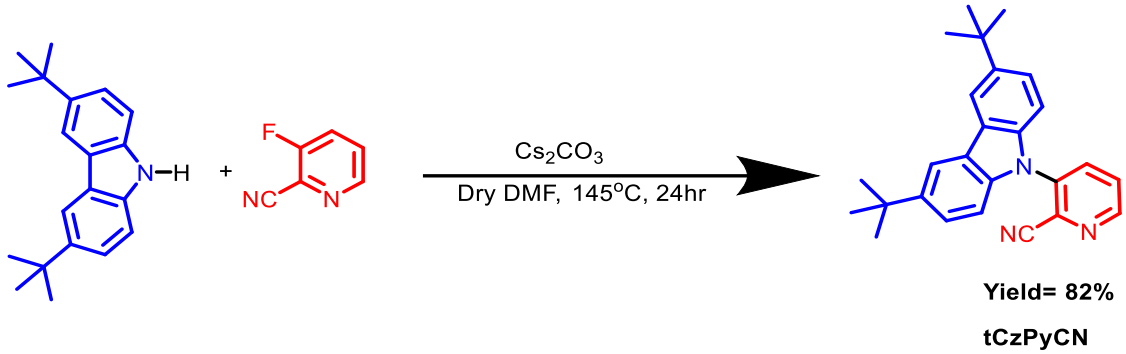

Scheme 1: Synthesis scheme of 3-(3,6-di-tert-butyl-9H-carbazol-9-yl)picolinonitrile (tCzPyCN)

2.2 Synthesis of 5,5'-bis(3,6-di-tert-butyl-9H-carbazol-9-yl)-[3,3'-bipyridine]-6,6'-dicarbonitrile (2tCz2Py2CN).

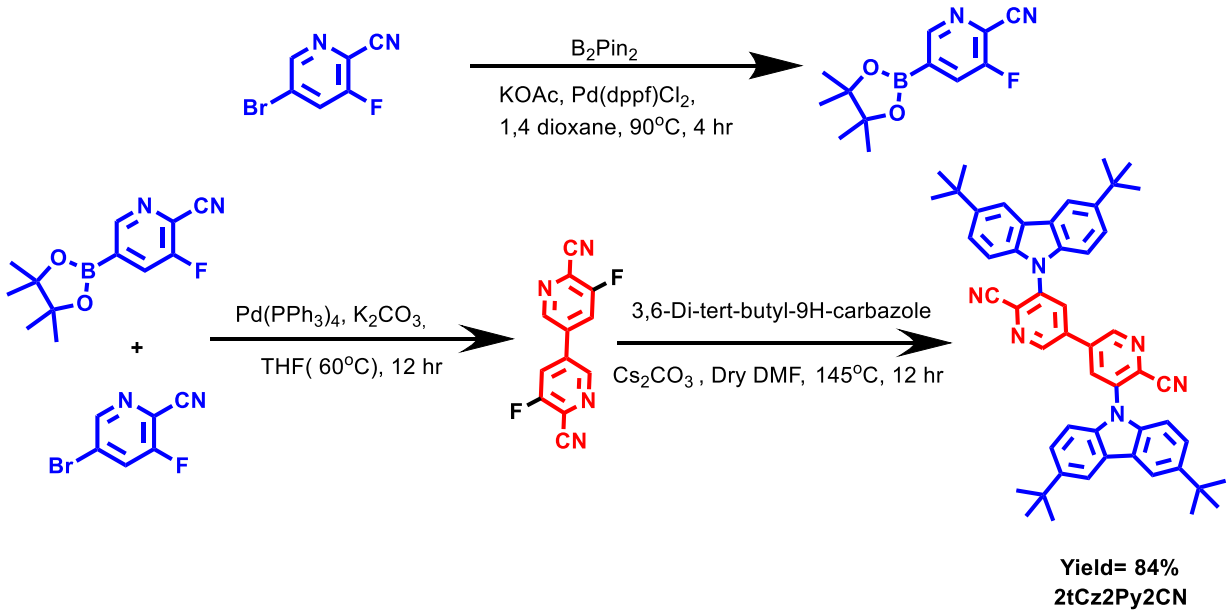

Scheme 2: Synthesis scheme of 5,5'-bis(3,6-di-tert-butyl-9H-carbazol-9-yl)-[3,3'-bipyridine]-6,6'-dicarbonitrile(2tCz2Py2CN).

Procedure: A mixture of 4,4,4',4',5,5,5',5'-octamethyl-2,2'-bi(1,3,2-dioxaborolane) (1 g, 3.90 mmol), [1,1'-bis(diphenylphosphino)ferrocene]dichloropalladium(II) (0.288 g, 0.39 mmol), potassium acetate (0.77 g, 7.87 mmol), in dry DMF 10 ml was placed in a 50 ml sealed tube under nitrogen environment. The reaction was stirred at 90 ºC for 24 h [Scheme 2]. The intermediate 3-fluoro-5-(4,4,5,5-tetramethyl-1,3,2-dioxaborolan-2-yl)picolinonitrile is not isolated and proceeded to the next step after filtration. After completion of the reaction, the mixture again charged with 5-bromo-3-fluoropicolinonitrile (1 eq.), tetrakis(triphenylphosphine) palladium(0) (10 mol%), K_2CO_3 (2 eq.) in THF and then nitrogen was purged followed by high vacuum, this was repeated three times and stirred at 70 ºC. After completion of the reaction, the mixture was extracted and dried using magnesium sulphate and then the solvent was removed under reduced pressure. The dried compound was then purified by silica gel column chromatography and eluted in 15% ethyl acetate/n-hexane mixture to give the desired white color 5,5'-difluoro-[3,3'-bipyridine]-6,6'-dicarbonitrile (FCNPyPyCNF) (yield=74%). Then finally, after the intermediate was isolated then FCNPyPyCNF (1.0 g, 4.60 mmol), tertiary butyl carbazole(tCz) (2.7 g, 9.66 mmol), cesium carbonate (3.15g, 9.66 mmol), we took and 20 ml dry DMF was injected in sealed tube and its was stirred at 145 ºC for 12 h. After completion of the reaction, the mixture was extracted and dried using magnesium sulphate and then the solvent was removed under reduced pressure. The dried compound was then purified by silica gel column chromatography and eluted in 10% ethyl acetate/n-hexane mixture to give the desired yellow color compound (yield=84%).^{1}H NMR (400 MHz, $CDCl_3$) of FCNPyPyCNF, δ 8.84 (s, 2H), 7.89 (d, J = 10.3 Hz, 2H), ^{1}H NMR (400 MHz, $CDCl_3$) of 2tCz2Py2CN, δ 9.06 (s, 2H), 8.16 (d, J = 16.9 Hz, 6H), 7.49 (d, J = 10.4 Hz, 4H), 7.16 (d, J = 8.6 Hz, 4H), 1.45 (s, 36H). ^{13}C NMR (400 MHz, $CDCl_3$) of FCNPyPyCNF δ 161.1 (d, J = 273.7 Hz), 145.15 (d, J = 4.6 Hz), 135.92 (d, J = 4.0 Hz), 123.84 (d, J = 15.4 Hz), 123.16 (d, J = 18.9 Hz), 112.28 (d, J = 5.1 Hz).^{13}C NMR (400 MHz, $CDCl_3$) of 2tCz2Py2CN, δ 147.57, 145.08, 139.93, 138.67, 135.24, 134.2, 133.21, 124.74, 124.38, 117.06, 114.92, 109.02, 34.91, 31.95. HRMS (ESI-QTOF) m/z: $[M+H]^+$ calculated for $C_{52}H_{52}N_6$ 761.4253, found 761.4230. m/z: $[M+H]^+$ calculated for $C_{12}H_{14}BFN_2O_2$ 249.1132, found 249.1186, m/z: $[M+H]^+$ calculated for $C_{12}H_4F_2N_4$ 243.0404, found 243.0482.

3. Computational Calculations

The molecular geometries, the ground-state (S_0) and lowest singlet excited state (S_1) geometries were optimized at the B3LYP/6-31G(d,p) level using the Gaussian g16[1] program package and

visualized using VMD.[1] The optimized result was in good agreement with the experimental findings. Frequency calculation was performed to obtain the lowest energy structure, and no imaginary frequency was obtained. The optimized S_0 state was used to determine the HOMO/LUMO distributions and dihedral angle(θ) tabulated below in Table S1. Based on the optimized configuration of S_0, oscillator strength (f), triplet spin density (TSDDs) and the excitation energy levels of the singlet and triplet states were computed using the TD-B3LYP/6-31G(d,p) the results are plotted below in Table S2. The Natural transition orbitals (NTOs) are visualized using the multiwfn[5] and summarized in Figure S1.

Table S1. Summary of the emitters showing theoretical values of both the emitters tCzPyCN and 2tCz2Py2CN at B3LYP/6-31G(d,p) level.

Compound	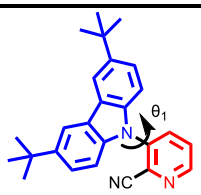 tCzPyCN	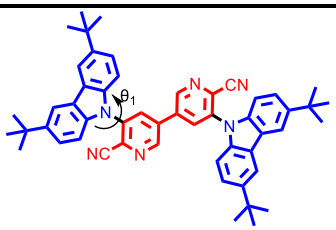 2tCz2Py2CN
HOMOs	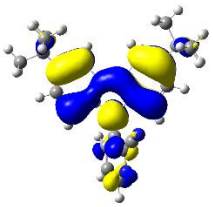 -5.52 eV	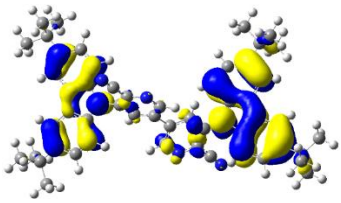 -5.67 eV
LUMOs	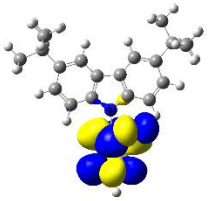 -1.95 eV	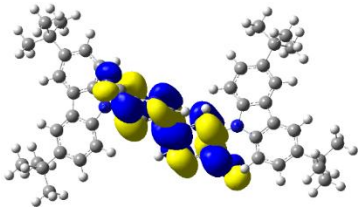 -2.80 eV
TSDDs (T_1)	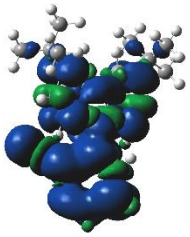	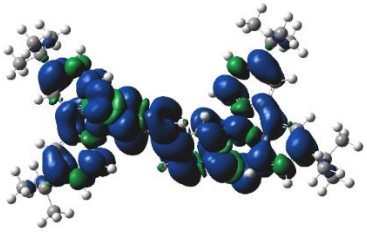

θ_1	64.1°	63.2°
S_1/T_1 (eV)	2.95/2.78	2.34/2.23
ΔE_{ST} (eV)	0.17	0.11

Table S2. Calculated excitation energies and orbital transitions for tCzPyCN and 2tCz2Py2CN using the B3LYP/6-31G(d,p) method.

tCzPyCN	**Excitation Energy/ eV**	**λ_{cal} (nm)**	**Oscillator Strength, f**	**Dominant excitation**
S_1	2.95	419.76	0.0224	HOMO → LUMO (99%)
S_2	3.33	371.93	0.0006	H-1 → LUMO (99%)
S_3	3.47	357.22	0.0761	HOMO → L+1 (98%)
T_1	2.79	444.77	0.0	HOMO → LUMO (92%)
T_2	3.12	396.81	0.0	H-1 → L+2 (51%)
T_3	3.16	391.99	0.0	HOMO → L+1 (71%)

2tCz2Py2CN	**Excitation Energy/ eV**	**λ_{cal} (nm)**	**Oscillator Strength, f**	**Dominant excitation**
S_1	2.3692	523.32	0.0333	HOMO->LUMO (95%) H-1->LUMO (3%)

S_2	2.3885	519.08	0.0031	H-1->LUMO (95%) HOMO->LUMO (3%)
S_3	2.7049	458.38	0.0018	H-2->LUMO (99%)
T_1	2.2508	550.84	0.0000	HOMO->LUMO (94%) H-6->LUMO (2%), H-1->L+3 (2%)
T_2	2.2759	544.78	0.0000	H-1->LUMO (95%) HOMO->L+3 (2%)
T_3	2.6921	460.55	0.0000	H-2->LUMO (97%)

Figure S1. Natural transition orbital of T_1 state of tCzPyCN and **2tCz2Py2CN** 2tCz2Py2CN at B3LYP/6-31G(d,p) level (isovalue=0.002)

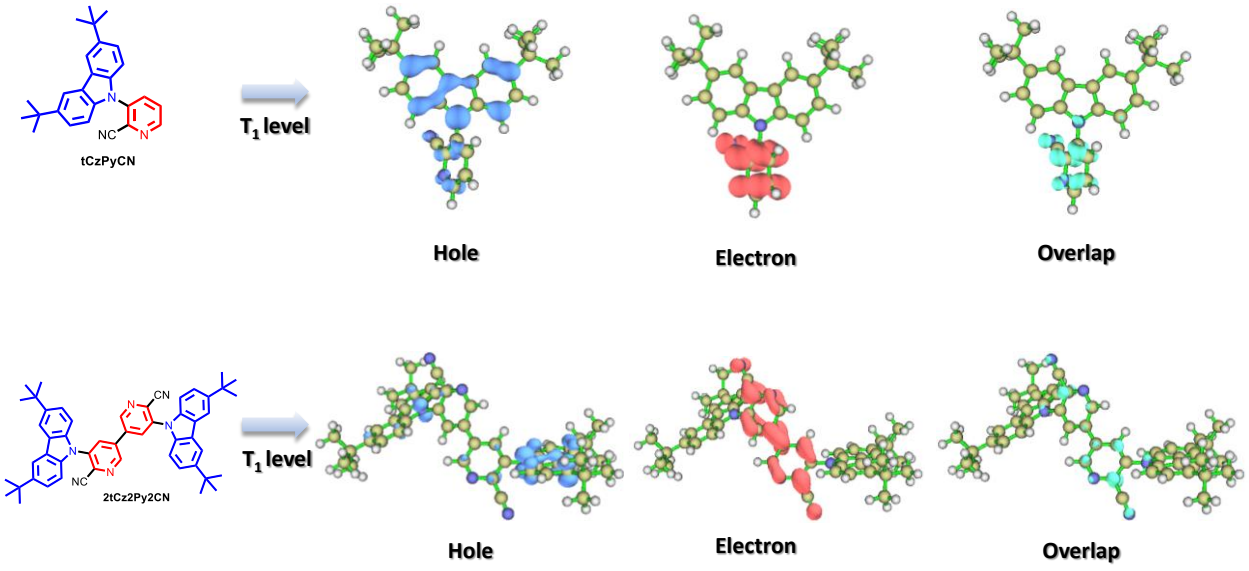

4. Photophysical properties

Table S3: The experimentally obtained parameters for the TADF emitters

Compound	λ_{abs} (ϵ_{max},$M^{-1}cm^{-1} \times 10^3$)[a]	λ_{em} (nm)[b]	E_S/E_T (eV)[c]	ΔE_{ST} (eV)[d]	HOMO/LUMO (eV)[e]	E_g (eV)[f]	T_{onset}[g]/T_g(^oC)[h]
tCzPyCN	318 (93), 331 (79), 375 (17)	444	3.25/3.04	0.21	-5.75/-2.65	3.1	269/-
2tCz2Py2CN	302 (89), 333 (72), 419 (11)	541	2.66/2.58	0.08	-5.77/-3.27	2.5	438/210

[a] For (1.0×10^{-5} M) Toluene solution. [b] For 5 wt.% doped film in mCBP. [c] Determined from the onset of fluorescence and phosphorescence spectra. [d] Experimental singlet–triplet energy gap. [e] HOMO and LUMO measured from the CV. [f] Optical band gap (E_g) determined form the intersection of absorption and emission wavelength. [g] Temperature corresponds to 5 wt.% loss (T_{onset}). [h] Glass transition temperature (T_g).

5. Equations for Calculating Photophysical Parameters of TADF Emitters.

$$1.\ k_p = \frac{1}{\tau_{PF}}$$

$$2.\ k_d = \frac{1}{\tau_{DF}}$$

$$3.\ k_r^S = \frac{\Phi_{PF}}{\tau_{PF}}$$

$$4.\ \Phi_{PF} = \frac{k_r^S}{k_r^S + k_{ISC}}$$

$$5.\ k_{RISC} = \frac{k_p \cdot k_d \cdot \Phi_{DF}}{k_{ISC} \cdot \Phi_{PF}}$$

$$6.\ k_{nr}^T = k_d - \phi_{PF} k_{RISC}$$

The above equations were utilized to calculate the rate constants, here $k_p, k_d, k_d, k_{ISC}, k_{RISC}$ and k_{nr}^T (assuming $k_{nr}^S \approx 0$)[6,7] are the rate constants of prompt fluorescence (PF), delayed fluorescence (DF), intersystem crossing and reverse intersystem crossing, respectively; k_r^s is the rate constants

of radiative transition from S_1 to S_0 respectively. k_{nr}^{T} is the non-radiative transition from the T_1 state. Φ_{PL}, Φ_{PF} and Φ_{DF} are the PLQYs of Total PLQY, PF and DF.[2]

6. Thermogravimetric Analysis (TGA) and Differential Scanning calorimetry (DSC)

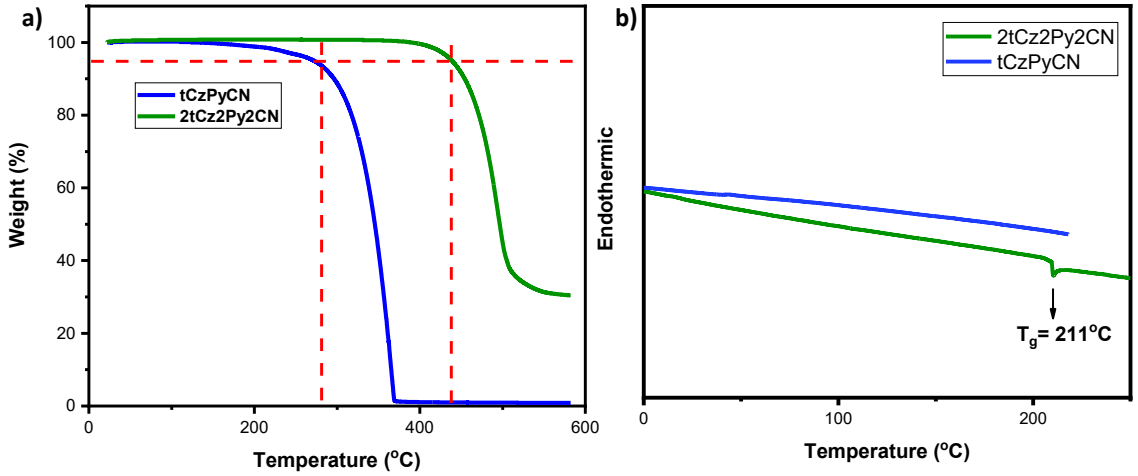

Figure S2. a) TGA, b) DSC of **tCzPyCN** and **2tCz2Py2CN** under N_2 at the rate of 10°C min^{-1}

7. Cyclic Voltammetry (CV)

Cyclic voltammetry (CV) was measured by using electrochemical analyzer with standard one-compartment, three-electrode electrochemical cell. The working electrode was a glass-carbon disk electrode. The counter electrode was a Pt wire. The reference electrode was Ag/AgCl. Ferrocenium/ferrocene (Fc^+/Fc) redox couple was used as the internal standard and the formal potential of Fc^+/Fc was 4.8 eV below vacuum. All potentials relative to Ag/AgCl electrode obtained from CV measurement were eventually referenced against Fc^+/Fc to calculate HOMO/LUMO levels. The HOMO/LUMO levels are calculated according to the following formalism:

$$HOMO = -(E_{ox} - Fc^{+}/Fc + 4.8)\ eV$$

$$LUMO = -(E_{red} - Fc^{+}/Fc + 4.8)\ eV$$

where the E_{ox} vs. Fc^+/Fc and E_{red} vs. Fc^+/Fc were oxidation and reduction onset potentials relative to Fc^+/Fc reference, respectively.

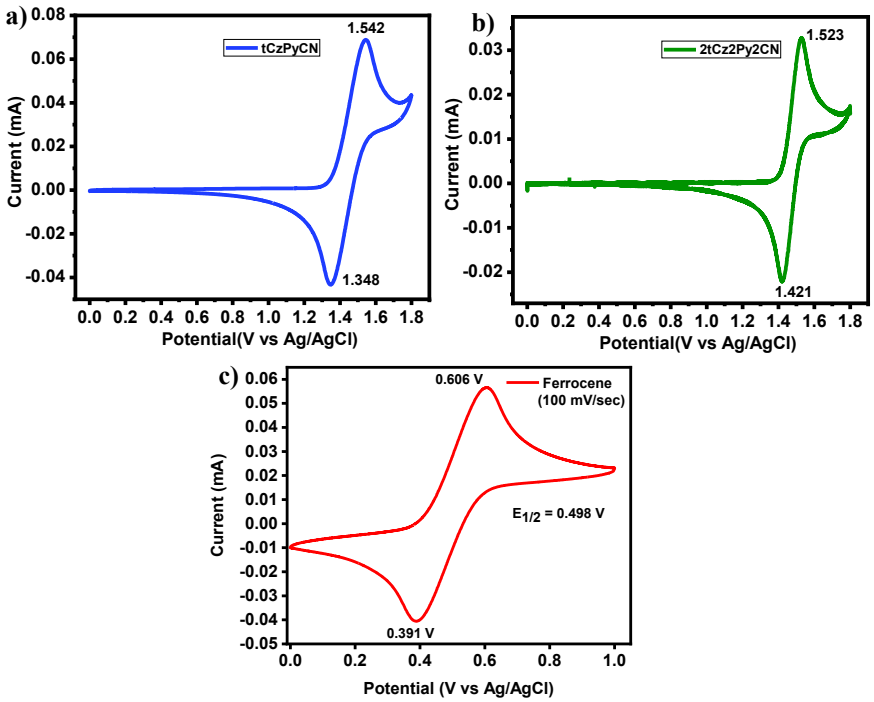

Figure S3. CV voltammograms of a) **tCzPyCN**, b) **2tCz2Py2CN** and c) Ferrocene in deoxygenated dichloromethane (DCM) with 0.1 M tetrabutylammonium hexafluorophosphate (TBAP) as supporting electrolyte.

8.Solvatochromism

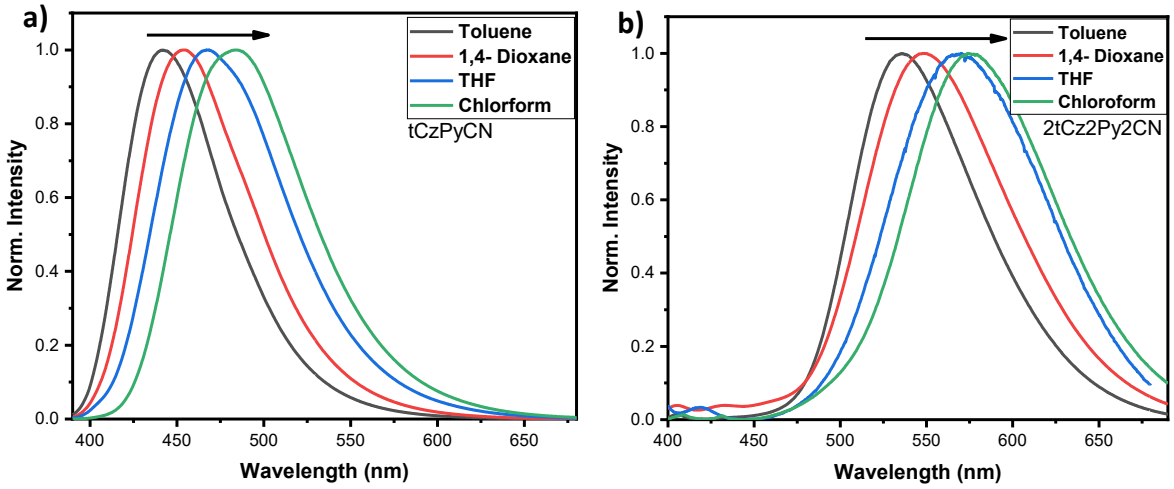

Figure S4. Excited state solvatochromism of a) tCzPyCN b) 2tCz2Py2CN with excitation wavelength (λ_{exc} = 375 nm) in Toluene, 1,4-Dioxane, THF and Chloroform.

9. UV-vis spectra of donor, intermediate and final emitter

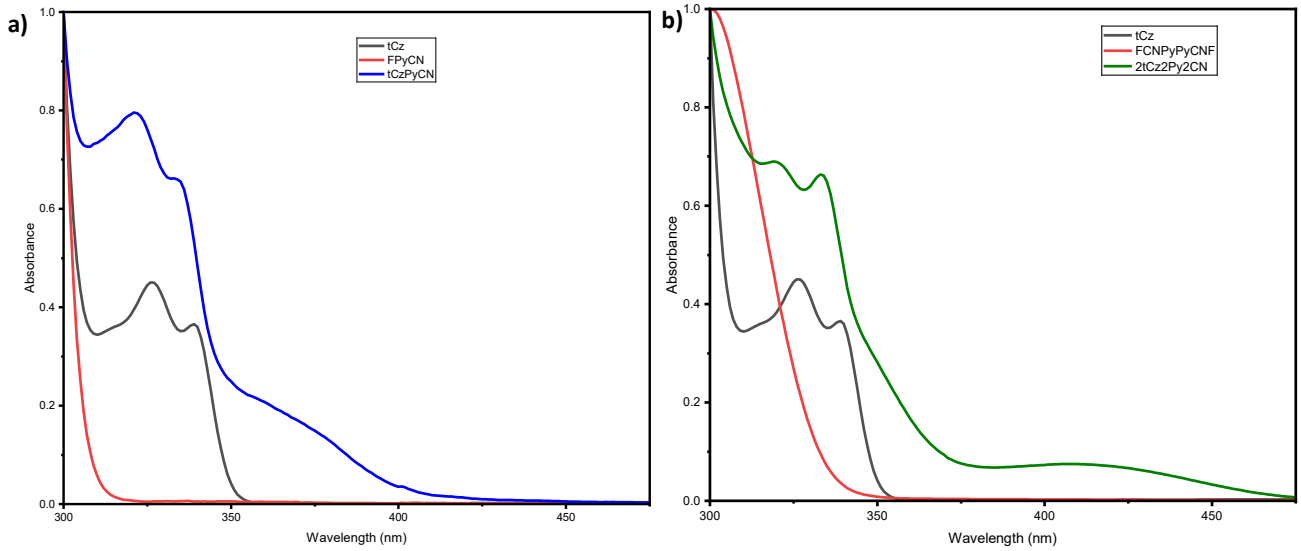

Figure S5. UV-vis of the precursors and intermediate of the emitter a) tCzPyCN b) 2tCz2Py2CN with excitation wavelength (λ_{exc} = 375 nm) in Toluene solution (10^{-5} M).

10.Device Fabrication and Characterization

Figure S6. a) Optimized device energy level structure for **tCzPyCN** and **2tCz2Py2CN** b) Molecular structure of the materials employed in the device c) Current-density-voltage-luminance(J-V-L) characteristics of tCzPyCN and 2tCz2Py2CN.

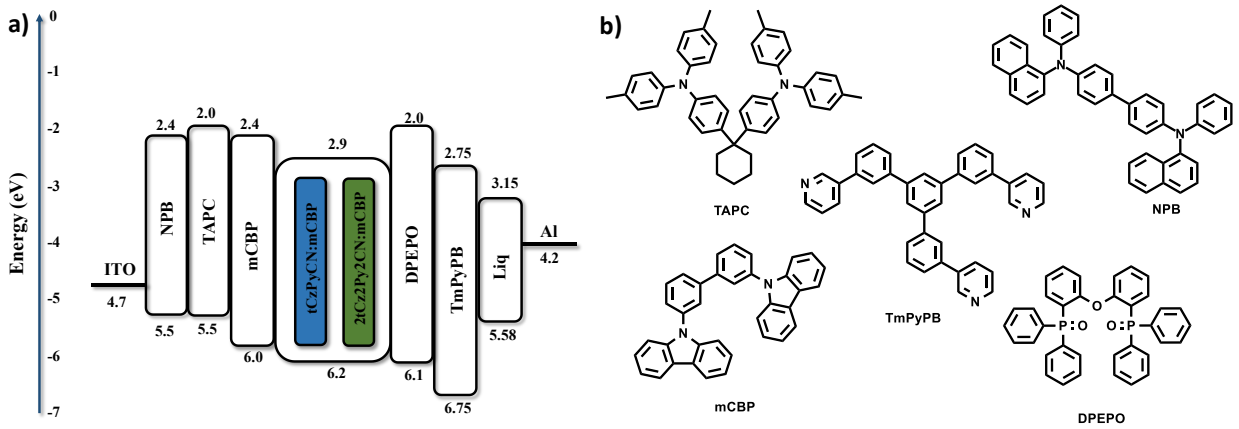

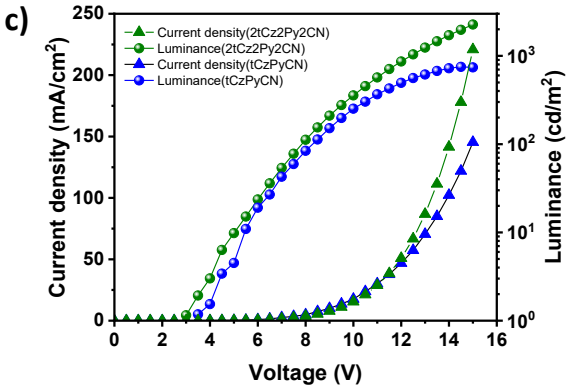

Table S4. Electroluminescence performance of the emitters tCzPyCN and 2tCz2Py2CN.

Emitter	[a]CD (mA/cm^2)	[b]L_{max} (cd/m^2)	[c]EL_{max}/FWHM (nm)	[d]EQE_{max} (%)	[e]PE_{max} (lm/W)	[f]CE_{max} (cd/A)	[g]CIE (x,y)
tCzPyCN (D1)	145	741	438/75	0.94	1.06	1.69	(0.16, 0.12)
2tCz2Py2CN (D2)	220	2263	535/97	15.02	40.98	52.18	(0.36, 0.57)

Device configuration: ITO/ NPB (30 nm)/ TAPC (20 nm)/ mCBP (5 nm)/ EML 5 wt.% tCzPyCN: mCBP= 15 nm, (5 wt.% 2tCz2PyCN: mCBP= 15 nm/ DPEPO (5 nm)/ TmPyPB (60 nm)/ Liq (2 nm)/ Al (100 nm), [a] Current density measured at 15 V [b] Maximum luminance. [c] Electroluminescence maximum. [d] Maximum external quantum efficiency EQE_{max} [e] Maximum power efficiency. [f] Maximum current efficiency. [g] Commission Internationale de l'Éclairage (CIE) coordinates.

11. NMR Spectra

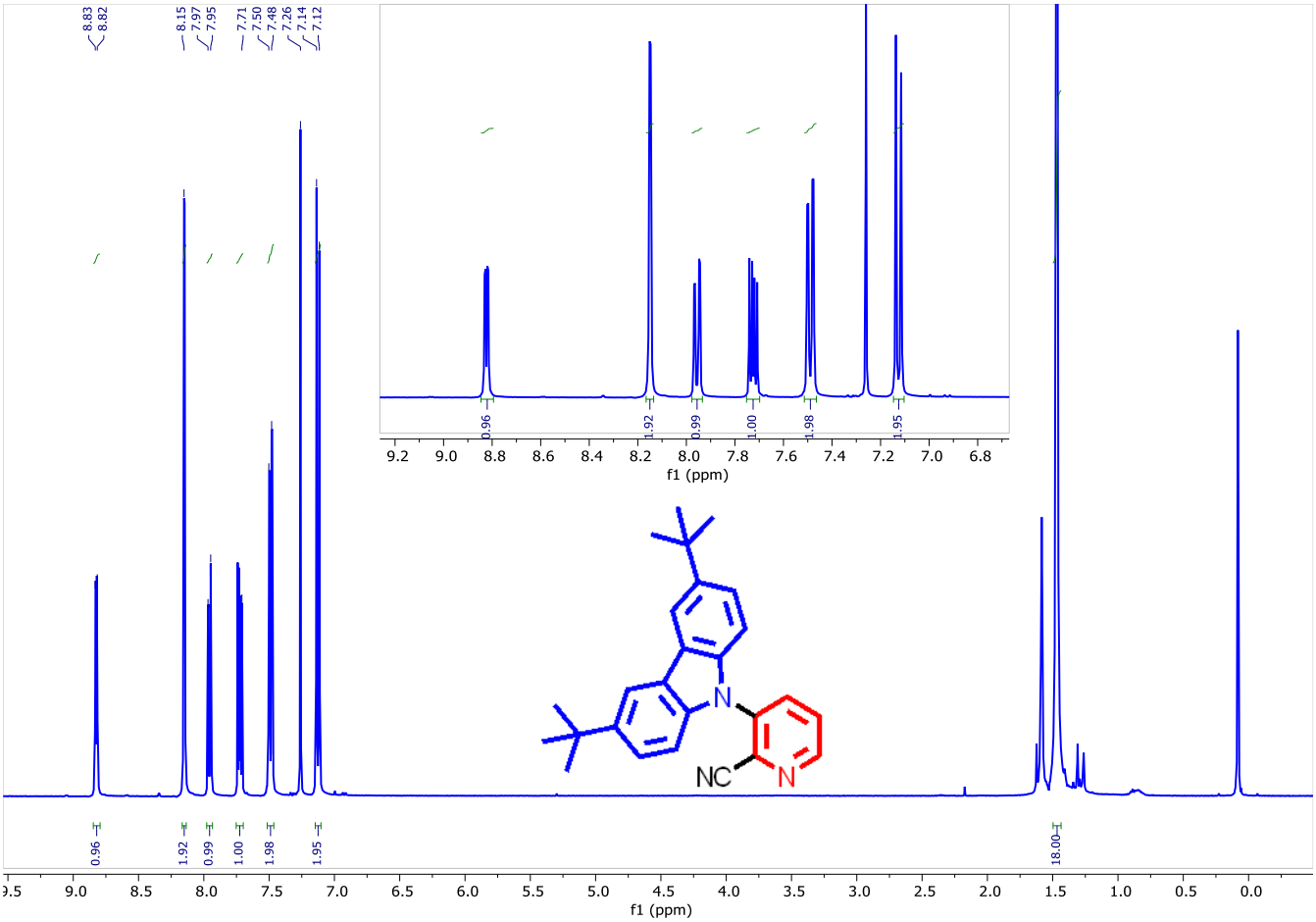

Figure S7. The ^{1}H NMR spectrum of **tCzPyCN** in $CDCl_3$.

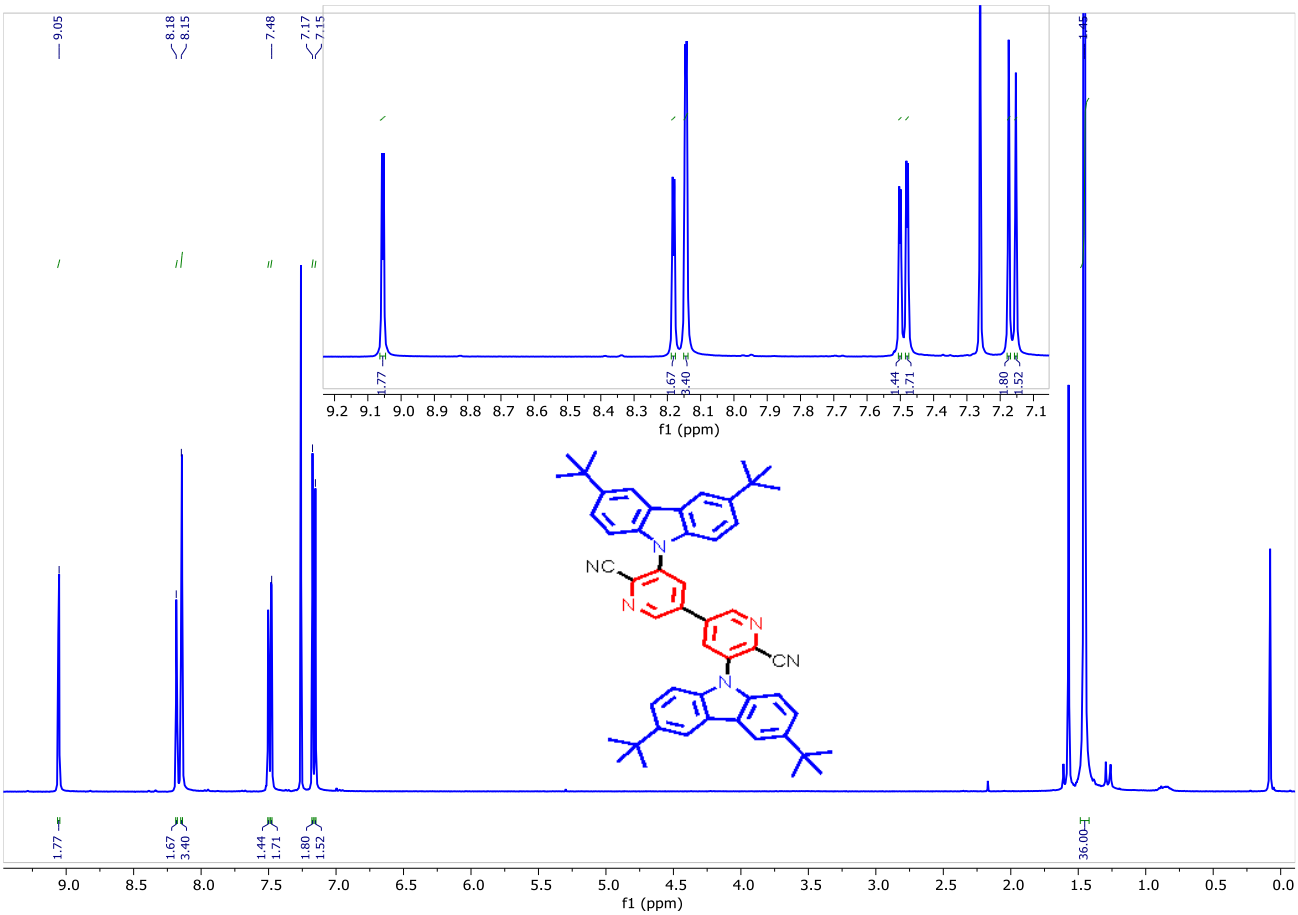

Figure S8. The ^{1}H NMR spectrum of **2tCz2Py2CN** in $CDCl_3$.

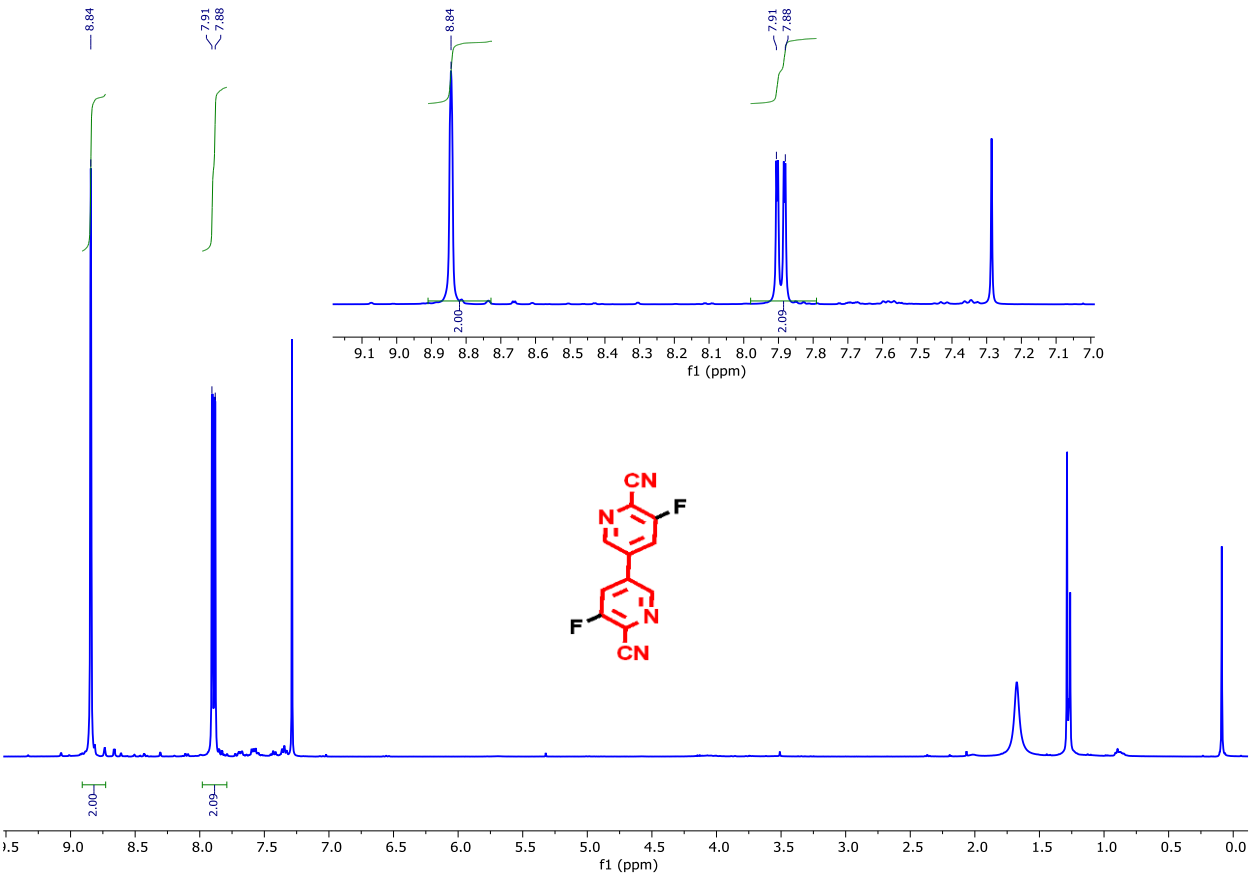

Figure S9. The ^{1}H NMR spectrum of **FCNPyPyCNF** in $CDCl_3$.

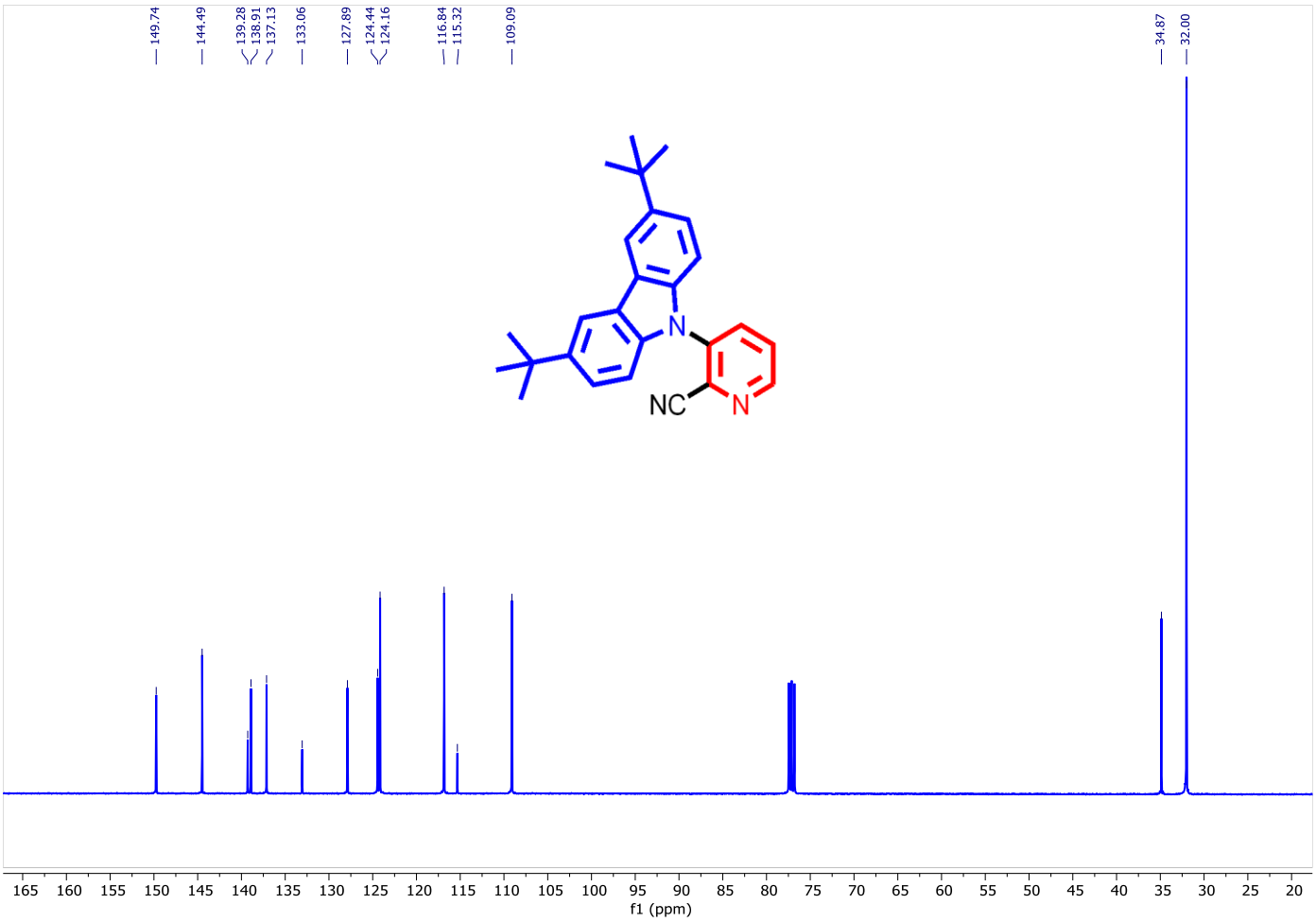

Figure S10. The ^{13}C NMR spectrum of **tCzPyCN** in $CDCl_3$.

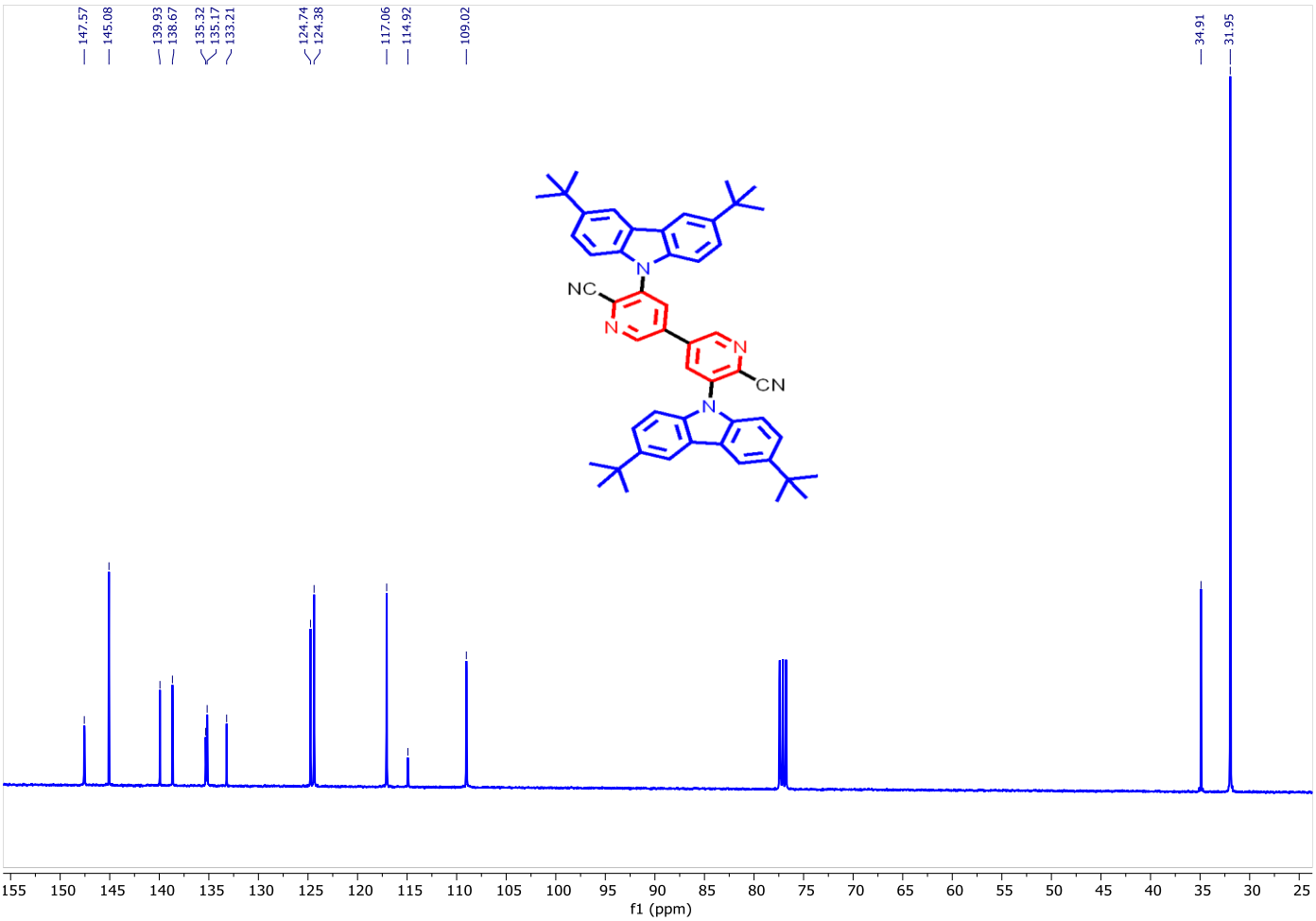

Figure S11. The ^{13}C NMR spectrum of **2tCz2Py2CN** in $CDCl_3$.

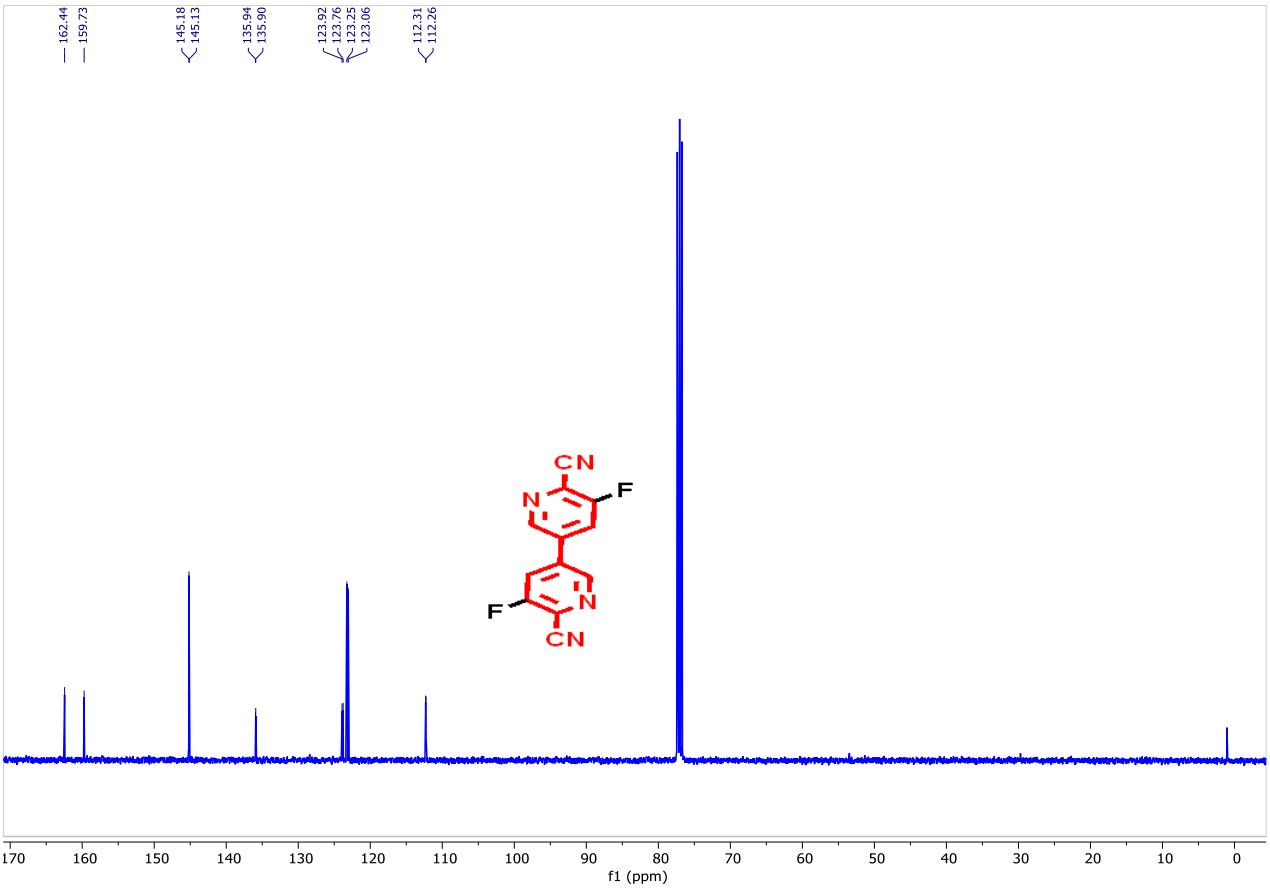

Figure S12. The ^{13}C NMR spectrum of **FCNPyPyCNF** in $CDCl_3$.

12. HRMS

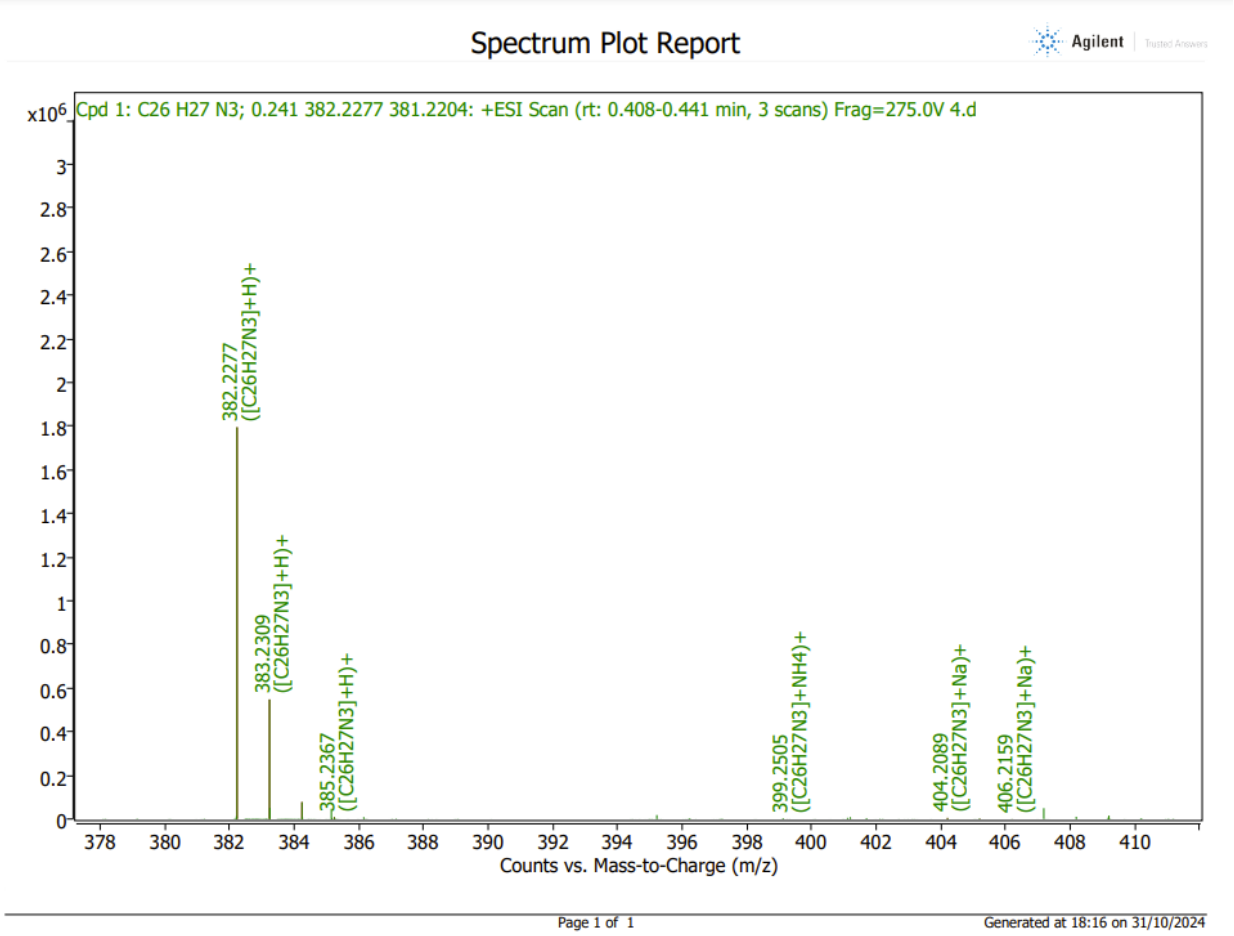

Figure S13. HR-MS spectrum of **tCzPyCN**.

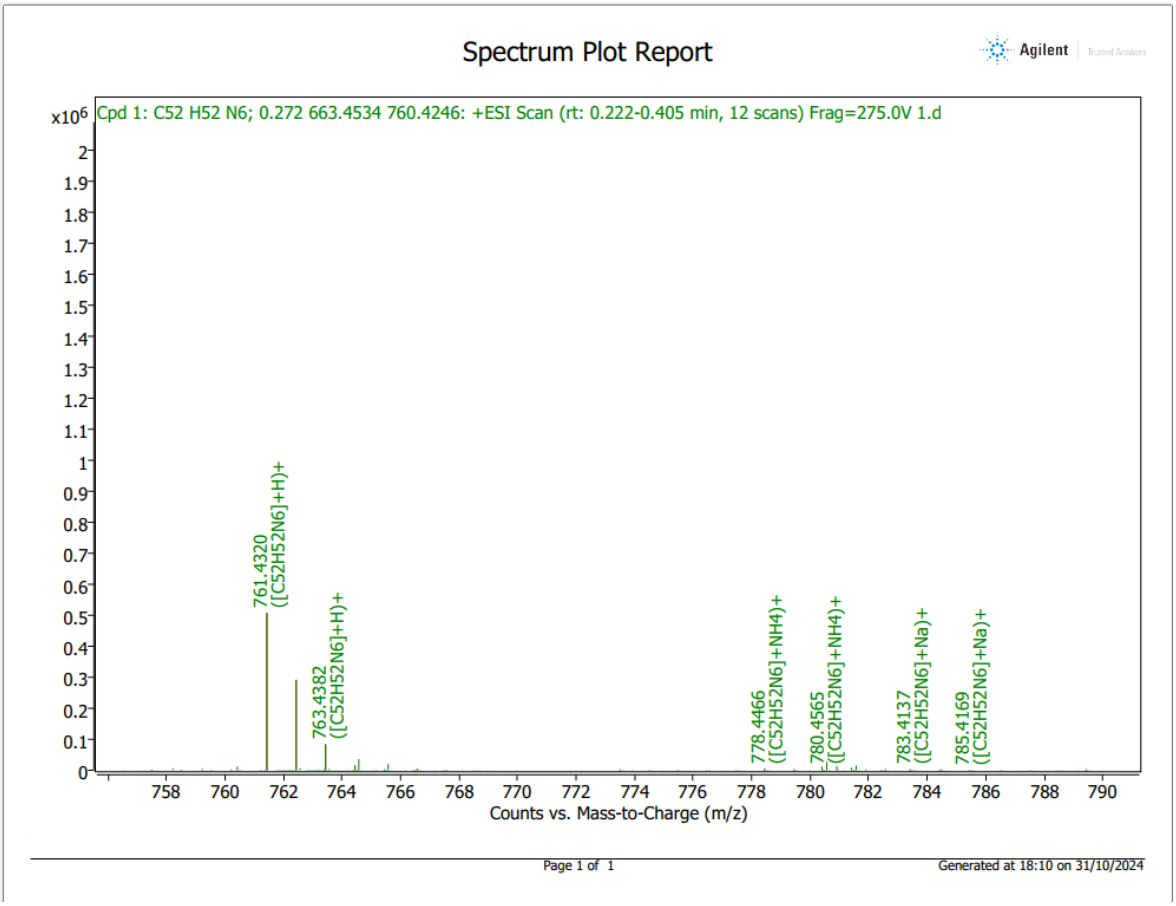

Figure S14. HR-MS spectrum of **2tCz2Py2CN**.

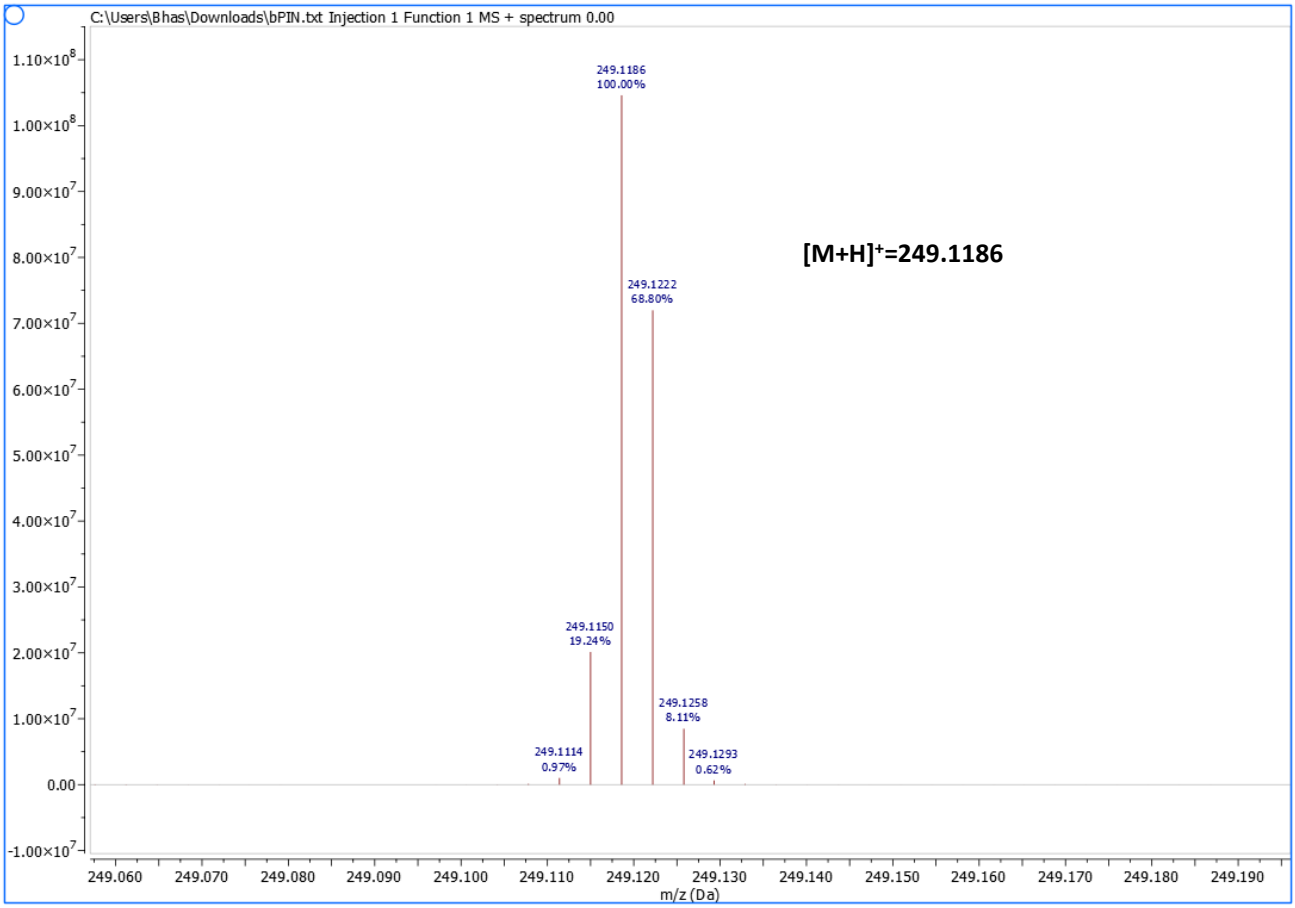

Figure S15. HR-MS spectrum of **3-fluoro-5-(4,4,5,5-tetramethyl-1,3,2-dioxaborolan-2-yl)picolinonitrile.**

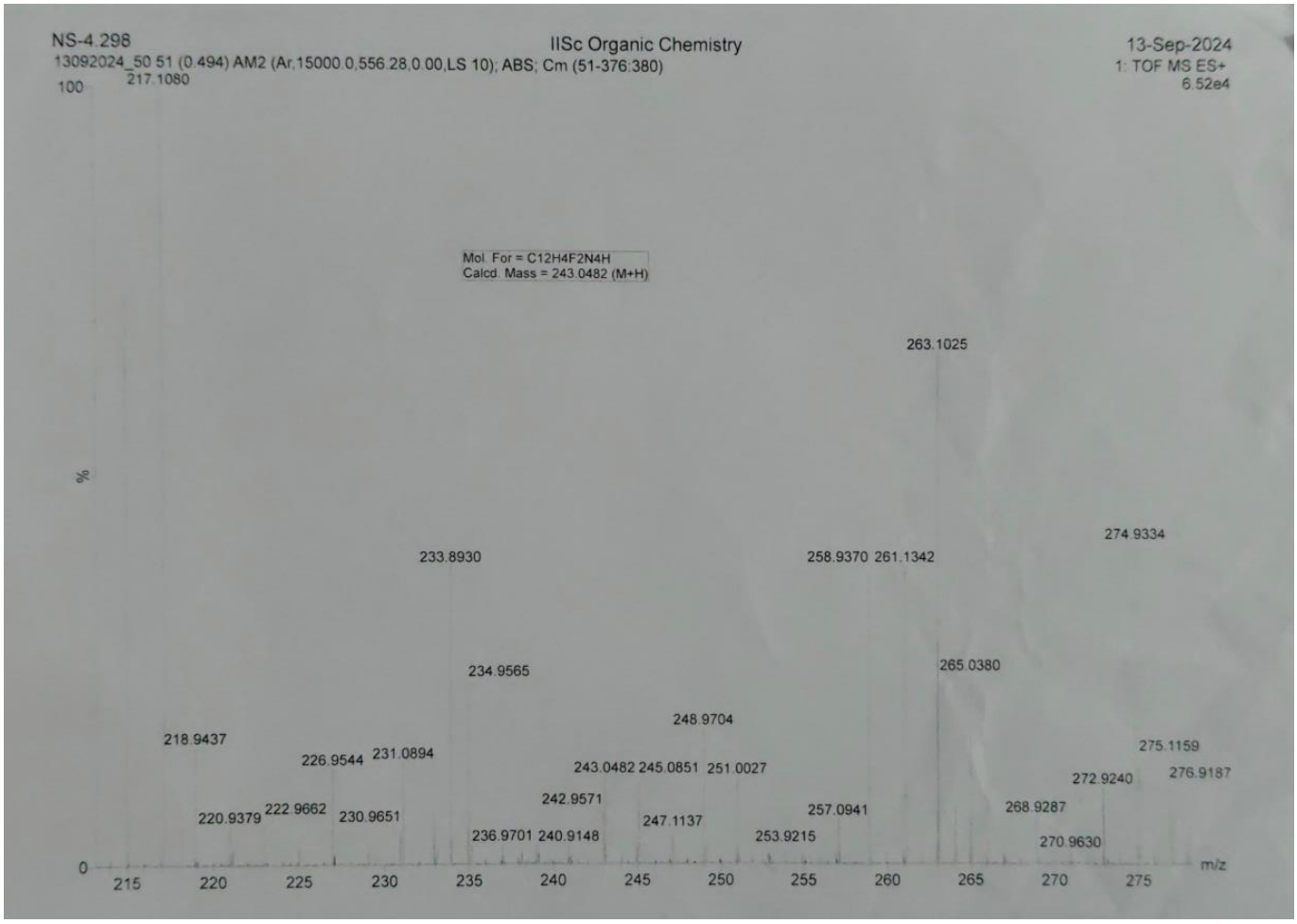

Figure S16. HR-MS spectrum of **FCNPyPyCNF**.

13. References

[1] M. J. Frisch, G. W. Trucks, H. B. Schlegel, G. E. Scuseria, M. A. Robb, J. R. Cheeseman, G. Scalmani, V. Barone, G. A. Petersson, H. Nakatsuji, X. Li, M. Caricato, A. V. Marenich, J. Bloino, B. G. Janesko, R. Gomperts, B. Mennucci, H. P. Hratchian, J. V. Ortiz, A. F. Izmaylov, J. L. Sonnenberg, Williams, F. Ding, F. Lipparini, F. Egidi, J. Goings, B. Peng, A. Petrone, T. Henderson, D. Ranasinghe, V. G. Zakrzewski, J. Gao, N. Rega, G. Zheng, W. Liang, M. Hada, M. Ehara, K. Toyota, R. Fukuda, J. Hasegawa, M. Ishida, T. Nakajima, Y. Honda, O. Kitao, H. Nakai, T. Vreven, K. Throssell, J. A. Montgomery Jr., J. E. Peralta, F. Ogliaro, M. J. Bearpark, J. J. Heyd, E. N. Brothers, K. N. Kudin, V. N. Staroverov, T. A. Keith, R. Kobayashi, J. Normand, K. Raghavachari, A. P. Rendell, J. C. Burant, S. S. Iyengar, J. Tomasi, M. Cossi, J. M. Millam, M. Klene, C. Adamo, R. Cammi, J. W. Ochterski, R. L. Martin, K. Morokuma, O. Farkas, J. B. Foresman, D. J. Fox, Wallingford, CT, **2016**.

[2] M. Du, M. Mai, D. Zhang, L. Duan, Y. Zhang, *Chem Sci.* **2024**, *15*, 3148-3154

[3] D. Volz, D. Zink and L. Bergmann (Cynora GmbH), *Ger. Offen.*, DE102016122122A1, **2017**.
[4] T. Lu, F. Chen, *J. Comput. Chem.*, **2012**, *33*, 580–592.
[5] H. Zhang, T. Huang, J. Zhou, C. Xu, D. Zhang and L. Duan, *Chem*, **2025**, 102685.
[6] M. Cai, M. Auffray, D. Zhang, Y. Zhang, R. Nagata, Z. Lin, X. Tang, C.-Y. Chan, Y.-T. Lee, T. Huang, X. Song, Y. Tsuchiya, C. Adachi and L. Duan, *Chem. Eng. J.*, **2021**, 420, 127591.
[7] S. H. Choi, C. H. Lee, C. Adachi and S. Y. Lee, *Dyes Pigm.,* **2019**, 171, 107775.
[8] M. Doi, H. Liu and S. Ando, *Polymer*, **2025**, 328, 128425.